

# Molecular docking, synthesis and biological evaluation of phenacyl derivatives of 9-aminoacridine as anti-Alzheimer's agent

**Rabya Munawar<sup>1,2\*</sup>, Nousheen Mushtaq<sup>1</sup>, Ahsaan Ahmad<sup>1,3</sup>, Syed Muhammad Ghufran Saeed<sup>6</sup>, Saman Usmani<sup>1,3</sup>, Shamim Akhtar<sup>4</sup>, ZS Saify<sup>5</sup>, Muhammad Arif<sup>4</sup> and Arifa Akram<sup>7</sup>**

<sup>1</sup>Department of Pharmaceutical Chemistry, Faculty of Pharmacy and Pharmaceutical Sciences, University of Karachi, Pakistan

<sup>2</sup>Department of Pharmaceutical Chemistry, Dow College of Pharmacy, Dow University of Health Sciences, Karachi, Pakistan

<sup>3</sup>Department of Pharmaceutical Chemistry, Institute of Pharmaceutical Sciences, Jinnah Sindh Medical University, Karachi, Pakistan

<sup>4</sup>Department of Pharmaceutical Chemistry, Faculty of Pharmacy, Hamdard University, Karachi, Pakistan

<sup>5</sup>HEJ Research Institute of Chemistry, University of Karachi, Karachi, Pakistan

<sup>6</sup>Department of Food Science and Technology, University of Karachi, Karachi, Pakistan

<sup>7</sup>Department of Pharmaceutical Chemistry, Faculty of Pharmacy, Federal Urdu University Arts, Science and Technology, Karachi, Pakistan

**Abstract:** Alzheimer's disease (AD) is a multifactorial neurodegenerative disorder mainly characterized by progressive deterioration of memory and impaired cognitive function. The most promising approach for symptomatic relief of AD is to inhibit acetylcholinesterase (AChE). On the basis of this approach in-house library of 9-aminoacridine derivatives were constructed and allowed to docked against human acetylcholinesterase (hAChE) (PDB ID: 4EY7), using MOE 2018.01 and PyRx 0.9.2 (AutoDock Vina). Top ranked and best fitted molecules were synthesized by targeting the 9-amino group of aminoacridine with substituted phenacyl halides. Anti-Alzheimer's potential was checked by in vitro AChE inhibition, antioxidant activity (DPPH scavenging ability) and fibril disaggregation. Subjected ligands suggested as promising multitargeted candidate with pronounced results in term of IC<sub>50</sub> values (AChE inhibition 2.400-26.138 $\mu$ M), however, none of them showed potential towards fibril inhibition.

**Keywords:** 9-Aminacridine, Alzheimer's disease (AD), acetylcholinesterase (AChE), molecular docking, MOE, PyRx (AutoDock Vina), AChE inhibition, antioxidant activity, Fibril disaggregation.

## INTRODUCTION

Alzheimer's disease (AD) is an age related progressive neurodegenerative process characterized by a gradual decline of cognitive and intellectual abilities. As the disease progresses with extensive failure of cholinergic neurons in various parts of the brain, languages and executive functions decline, disorientation and non-cognitive symptoms such as psychiatric, behavioral, motor and sensory disturbances can emerge (Alzheimer's Association, 2017; Acosta *et al.*, 2017; Aouani *et al.*, 2017; Fernandez *et al.*, 2017; Gensicka-Kowalewska *et al.*, 2017; Kristofikova *et al.*, 2017; Peauger *et al.*, 2017; Yang *et al.*, 2019).

AD pathogenesis has not been clarified yet but decreased level of acetylcholine (ACh, neurotransmitter) by huge loss of cholinergic neurons, plays a critical role in the progression of AD because it involve in cognitive mechanism. Low level of ACh, oxidative stress, accumulation of  $\beta$ -amyloid and tau protein, dyshomeostasis of biometals and inflammatory responses are major factors in pathophysiology of AD (Spilovska *et al.*, 2013; Ambure *et al.*, 2014; Brogi *et al.*, 2014; Bacalhau *et al.*, 2016; Chen *et al.*, 2016; Cavdar *et al.*, 2019; Jannat *et al.*, 2019).

\*Corresponding author: e-mail: pharmacistrabya@gmail.com

Acetylcholine is rapidly hydrolyzed in the synaptic space by the acetyl cholinesterase into acetic acid and choline, thus, inhibition of this particularly enhance intellectual activity by increasing neurotransmission of cholinergic synapses in the brain. While this strategy works in patients with AD but curative therapy still an unachieved goal (Aksu *et al.*, 2016; Cavdar *et al.*, 2019; Cheng *et al.*, 2017; Gensicka-Kowalewska *et al.*, 2017; Gocer *et al.*, 2015; Inestrosa *et al.*, 2008; Johnson & Moore, 2006; Tiwari *et al.*, 2013; Weinstock & Groner, 2008). With low recovery rate, AD has attracted the attention of medical chemists, who have studied new drugs for the cure of this disease. Tacrine, donepezil, galantamine, rivastigmine and memantine are Food and Drug Administration (FDA) approved drugs, useful in only definite symptomatic (mild to moderate) improvement in memory and cognitive function but unable to stop the progressive neurodegeneration in AD (Anand and Singh, 2013; Ambure *et al.*, 2014; Bacalhau *et al.*, 2016; Nwidu *et al.*, 2017; Chen *et al.*, 2019; Yang *et al.*, 2019). During the past few years usage of these drugs has been limited because of their side effects like gastrointestinal disturbances and hepatotoxicity (Ado *et al.*, 2015; Senol *et al.*, 2011). Due to this reason the development of nontoxic cholinesterase inhibitors (ChEIs) are great interests among researchers. In recent years, the need of disease modifying drugs for AD has been addressed via new approaches. Although in order to design structures

for multitarget directed ligands (MTDLs) with multifactorial and compel etiology of AD to produce the desired therapeutic efficacy, these methods has been used (Jannat *et al.*, 2019).

9-amino moiety with a multisubstituted variety of functional groups produced substantial impact on their biological activities along with neurodegenerative diseases like AD and provided solid background for 9-aminoacridine-based compounds synthesis, structure activity relationship (SAR) and biological activity (Borovlev *et al.*, 2016; Gellerman 2012; Manivannan *et al.*, 2012). Tacrine is the first derivative of 9AA that is identified and used in medicine as an effective anti-AD drug (Korabecny *et al.*, 2010).

The design and discovery of new medicinal agents has now shifted from the scientific laboratory to the computer by the use of computational method like computer aided drug design (CADD). It is very cost effective in research and development and can bridge almost all stages of drug discovery i.e., from the identification of target with lead discovery, optimization of lead compound to clinical trials. Docking is a part of molecular modeling; allow the ligand to fit into its pocket site to specify its binding potential (Begum *et al.*, 2018; Christoph *et al.*, 2004; Lopez-Vallejo *et al.*, 2011; Meng *et al.*, 2011; Rahman *et al.*, 2012; Scotti *et al.*, 2018).

Pursuing our efforts in designing new 9-aminacridine derivatives as antialzheimer's agents by evaluating their *insilico* and *in vitro* AChE inhibitory properties, we identified potential compounds. However, its activity profiling towards antioxidant and fibril disaggregation were also conducted. These activities determine the efficacy of these compounds to work as multi-target drugs.

## MATERIAL AND METHODS

### General

All reagents and chemicals were purchased from Merck and Sigma-Aldrich (Germany). All solvents were of reagent grade and distilled twice before use. TLC plates with silica gel 60 GF<sub>254</sub> were used to monitor the progress of the reactions and check the purity of the chemicals. TLC spots were visualized at 254 and 365nm on HP-UVIS Desaga (Heidelberg, Germany). STUART melting point apparatus (U.S.A) used for melting point determination and spectroscopic data were recorded on Shimadzu UV-visible (UV-1601, Japan), ALPHA II FTIR (Bruker, Germany) and nuclear magnetic resonance (<sup>1</sup>H-NMR) in d<sub>6</sub>-DMSO and deuterated methanol (MeOD) on Bruker Advance AV-400 and AV-500 MHz, France. Molecular mass recorded on Fast Atomic Bombardment (FAB) technique (JEOL 600H-2, U.S.A).

### Molecular Docking

X- ray crystallographic structure of human acetyl cholinesterase (hAChE) (PDB ID: 4EY7, resolution: 2.35 Å) was retrieved from virtual protein databank (PDB) ([www.rcsb.org](http://www.rcsb.org)). 4EY7 based on chain A and B with 524 amino acids (Sukumaran *et al.*, 2018). Chain B has attached standard donepezil was selected for *insilico* studies. For AutoDock Vina, the preparation of receptor protein involved the removal of excess charges, non-essential molecules of water and non-bonded inhibitors, however, addition of polar hydrogens and merging of non-polar ones was done by Chimera 1.10.2, UCSF Chimera molecular visualization application. Gasteiger charges were assigned to all atoms and protein was allowed to relax fully by selecting 1000 descent steps and saved in pdb.

In MOE, dimeric chain was refined for clashes and used only monomer. All water molecules and heteroatoms (except donepezil) were removed for visualization ease. However, hydrogen atom/s, missing residues and partial charges were added by using Quickprep of MOE to simulate the system with normal human physiology. Moreover, energy minimization of target protein was carried out under MMFF94x force field (Halgren, 1996; Halgren, 1999) and the active sites was located via MOE alpha site finder.

A virtual library of proposed 9-aminacridine compounds with structural diversity has been sketched using ChemDraw Ultra 8.0, followed by their compatibility to molecular environment using OpenBable. Biologically known compounds were retrieved from PubChem database (<http://www.ncbi.nlm.nih.gov/pccompound/>) to be included in dataset for comparison. The library was then subjected to protonation and energy minimization for their geometry optimization using MMFF94 with optimization algorithm conjugate gradients and 1000 number of steps for attaining least energy conformations and stored as pdb files.

Before starting, validation of molecular docking was performed to check the reproducibility of software for particular biological system. MOE DOCK module was used under a defined force field and rescoring. The cognate ligand molecule (E20) using alpha site finder module and to confirm the parameters, re-docked on 4EY7.pdb showed a root mean square deviation (RMSD) <1 Å, signifying appropriate method robustness.

Molecular docking studies were performed on PyRx0.9.2 software package (Jacob *et al.*, 2012; Muhammad & Fatima, 2015). For docking, both Macromolecule and ligands were converted into pdbqt. The active site was specified by generating a centroid grid box, following xyz coordinates were applied: that range widely for hAChE in three directions (10.698, -58.115, -23.192). Molecular

docking was carried out in Vina Wizard (PyRx-Virtual Screening Tool-Version 0.9.2) program utilizing computer resources.

Two-steps calculation was proceed with Proxy Triangle placement algorithm, Alpha HB scoring and GBVI/WSA rescoring methods through induced fitting of molecules. In first step, without energy minimization docking was carried out only to find whether in-house library will bind to an active pocket or not, however, in the next step specific docking with all statistics and ligands at their energy minima was run to determine their binding energies.

#### **General Procedure for synthesis of 9-Aminoacridine Derivatives**

A mixture of tetrahydrofuran (THF) based solution of 9-aminoacridine (0.0025M) and phenacyl halides (0.0025M) were stirred at room temperature (rt) for 5-25hours at alkaline pH and refluxed at 50°C for 15-20 hours. Reactions were monitored and confirmed by TLC using solvent system of ethanol and chloroform with few drops of ethyl acetate. After cooling, the resulting product [Scheme 1 & 2] precipitates were collected by filtration under reduced pressure, washed with THF, recrystallized by THF and alcohol and dried under vacuum over silica. Melting points were recorded and uncorrected.

#### **Acetylcholinesterase Inhibition**

Acetylcholinesterase inhibiting activity was performed on Spectronic 20D+ (Thermoscientific, USA) with slightly modification of Ellman method. Acetylcholinesterase (AChE, E.C. 3.1.1.7, lyophilized powder, electric eel,  $\geq 1000$  unit), acetylthiocholine iodide (ATCI) and 5,5-dithiobis-(2-nitrobenzoic acid) (DTNB) were purchased from Sigma-Aldrich (St. Louis. Mo, USA). Mixture of dimethyl sulfoxide (DMSO) and methanol (MeOH) in equal ratio were used to prepare test compounds and diluted in 0.1M potassium phosphate ( $\text{KH}_2\text{PO}_4/\text{K}_2\text{HPO}_4$ ) buffer of pH 8.0. Six different concentrations of each compound were tested in triplicate. Each sample mixture contained 50 $\mu$ l buffer (pH 8), 25 $\mu$ l test compound and 25 $\mu$ l enzyme (0.22U/ml in buffer) and at room temperature incubate for 15 min. Then add 125 $\mu$ l DTNB (3mM in buffer) and ATCI (3mM in water) and check hydrolysis of ATCI at 412nm spectrometrically after 15 min. The  $\text{IC}_{50}$  values were calculated along with control and blank run (Ellman *et al.*, 1961; Mohammadi-Khanapostani *et al.*, 2015).

#### **Antioxidant (DPPH Scavenging) activity**

2,2'-diphenyl-1-picrylhydrazyl (DPPH) 100 $\mu$ M was prepared in methanol. Test compounds prepared in different concentrations (0-200 $\mu$ M) in methanol mixed well with DPPH in equal volumes and kept in dark for 20 min. The absorbance (Abs) of this mixture was measured at 517 nm by spectrophotometer UV-1601, Shimadzu

(Japan). The following equation was used to calculate percentage scavenging:

$$\% \text{ Scavenging} = \frac{\text{Abs of blank} - \text{Abs of test}}{\text{Abs of blank}} \times 100$$

$\text{IC}_{50}$  was obtained from percent (%) scavenging. Ascorbic acid was used as standard. Experiments were performed in triplicate (Narla and Rao, 1995; Venkatachalam *et al.*, 2012).

#### **Fibrils Disaggregation**

Lyophilized powder of lysozyme from chicken egg white (CEW, lot number SLBT5160,  $\geq 90\%$ ,  $\geq 40,000$ units/mg protein, Sigma-Aldrich). Spectrophotometrically determine protein concentration at 280 nm using an extinction coefficient ( $\epsilon_{280}$ ) of  $2.65 \text{ Lg}^{-1} \text{ cm}^{-1}$ . Glycine buffer 100mM of pH 2 was prepared containing 100mM NaCl (50ml). 70 $\mu$ M Protein solution prepared in glycine buffer 10ml (final volume). Then protein solution incubated on shaking water bath SHZ-82 (China) at 75°C for 48 hours. The lysozyme amyloid aggregates were confirmed by measuring absorbance with Congo red (CR). The spectrum was recorded by Shimadzu UV-visible (UV-1601), Japan spectrophotometer from 400 to 700 nm. Freshly prepared 20 $\mu$ M CR in phosphate buffer 100mM (pH 7.4) mixed with 0.5ml prepared fibrils (protein solution) and 3ml CR solution and then recording the absorption spectrum after incubation (at least 30 min) along with CR alone as control at room temperature. Presence of fibrils will be characterized by peak shift from 492-512nm. Prepare drug sample solutions of different concentration in DMSO and 100mM glycine buffer. The stock solutions of drugs prepared freshly in DMSO. The volume of DMSO in measuring samples was lower than 2% then final volume makeup with 100mM glycine buffer. Take 0.5ml protein aggregates solution and add 0.5ml drug sample solution and leave for 24 hours. After that add 3ml 20 $\mu$ M Congo red solution in each drug and protein mixture as well as protein alone and incubate for at least 30minutes at room temperature. Now take UV absorption scan from 400-700nm. For disaggregation peak shift between 500 to 510nm (Gazova *et al.*, 2008; Ramshini *et al.*, 2015).

## **STATISTICAL ANALYSIS**

All the results of the in vitro tests were represented in  $\text{IC}_{50} \pm \text{S.D}$  (Standard deviation) calculated by Regression line formula, Microsoft Excel, Windows 8.1.

## **RESULTS**

Energy score and chemical interactions are mentioned in table 1 and figs. 1-4. Both compounds fit in to the active site targeting all essential areas on enzyme making hydrogen and hydrophobic interactions with all the important amino acid residues. MOE and Auto Dock Vina presented good number of hydrogen and hydrophobic

interactions between ligands and target. The minimum predicted Gibbs binding energy was taken as the top-scoring modes from the obtained results. Execution the graphic and visualization illustrations of 3D docked poses; GUI of Chimera 1.10.2 (<https://www.cgl.ucsf.edu/chimera/>) and MOE were utilized.

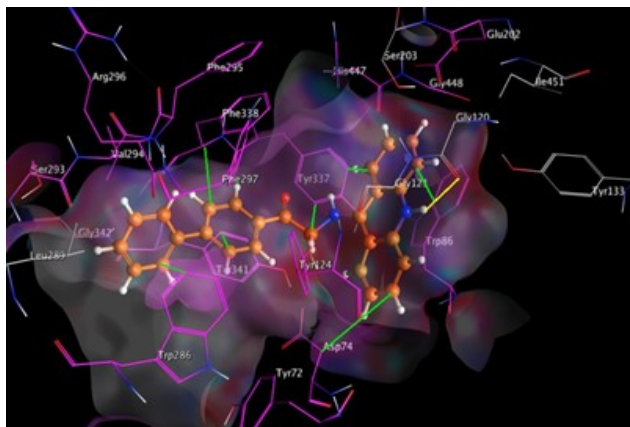


**Fig. 1:** 3D Good fit pose of PS12 in active site of AChE (MOE)

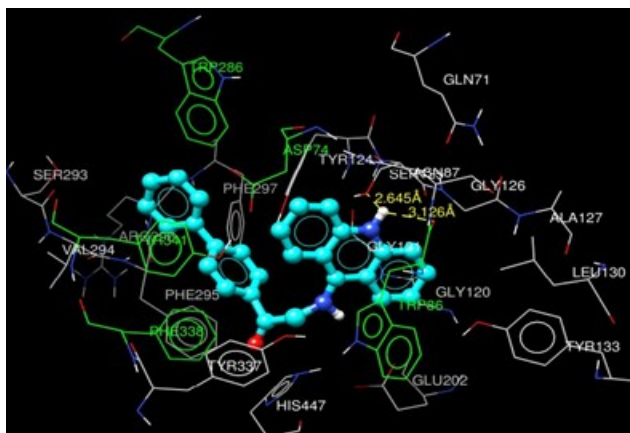


**Fig. 2:** 3D Good fit pose of PS12 in active site of AChE (Chimera)

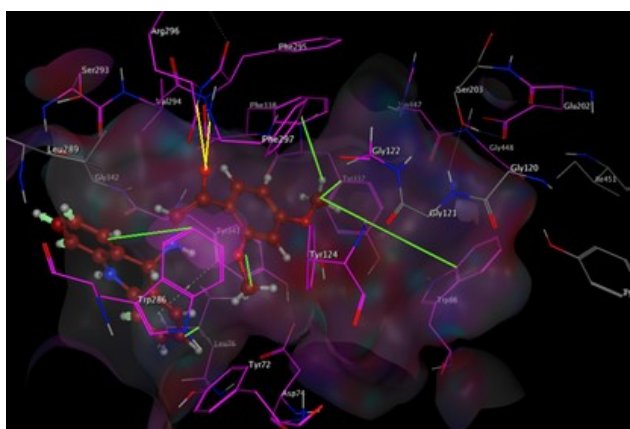


**Fig. 3:** 3D Good fit pose of PS13 in active site of AChE (MOE)

Selected compounds successfully synthesized by N alkylation of 9-aminoacridine and their structures were confirmed with the help of spectroscopic studies (Scheme 1 and 2). Results of AChE inhibition, antioxidant activity and fibril disaggregation shown in table 2. Both compounds revealed better enzyme inhibition and antioxidant activity as compared to parent and standards. PS12 showed better results than PS13. Compounds were unable to disaggregate the fibrils at the tested dose.

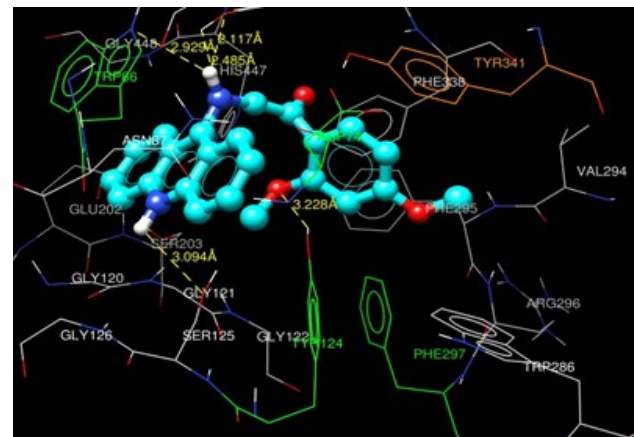


**Fig. 4:** 3D Good fit pose of PS13 in active site of AChE (Chimera)

### *N(4'-phenylphenacyl)-9-aminoacridine (PS12)*

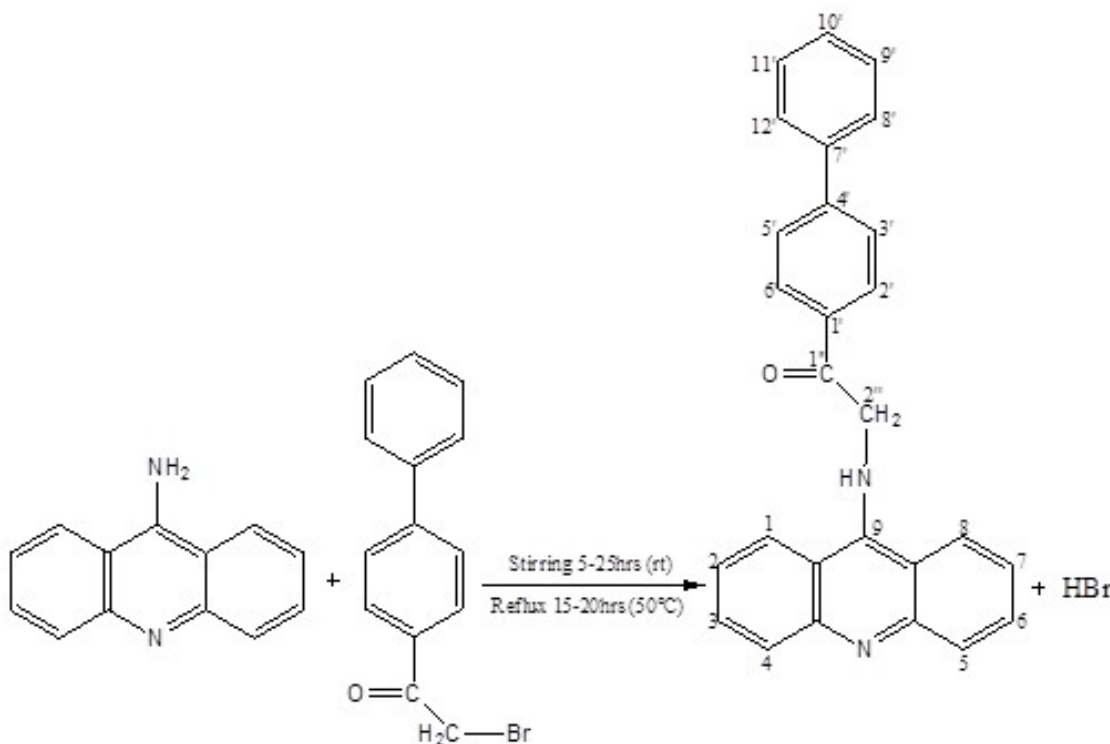
Crystalline yellow powder. Yield: 74.725%, melting Point decomposed 253°C. UV (MeOH)  $\epsilon$ : 8095.9032 mol<sup>-1</sup>cm<sup>-1</sup>, IR ( $\nu_{max}$ ) cm<sup>-1</sup>: 750, 1450, 1580, 1780, 3030 and 3100. FAB positive (m/z): 310. <sup>1</sup>H-NMR (MeOD, 500 MHz),  $\delta$ (ppm): 8.642-8.663 (d, 4H, H-4, 5, 2', 6'  $J$ =8.4Hz), 7.950-7.990 (t, 5H, H-2, 7, 9', 10', 11'  $J$ =16Hz), 7.531-7.568 (t, 4H, H-3, 6, 3', 5'  $J$ =14.8Hz), 7.877-7.898 (d, 4H, H-1, 8, 8, 12'  $J$ =8.4Hz), 2.486 (s, 2H, H-2").

### *N*(2',4'-dimethoxyphenacyl)-9-aminoacridine (PS13)

Crystalline yellow powder. Yield: 66.56%, melting point 170°C. UV (MeOH)  $\epsilon$ : 4031.77 mol<sup>-1</sup>cm<sup>-1</sup>, IR ( $\nu_{max}$ ) cm<sup>-1</sup>: 760, 1020, 1250, 1410, 1480, 1600, 1660, 3000 and 3080. FAB positive (m/z): 418. <sup>1</sup>H-NMR (d<sub>6</sub>-DMSO, 400 MHz)  $\delta$  (ppm): 3.872 (s, 3H, H-7'), 3.957 (s, 3H, H-8'), 4.717 (s, 2H, H-2''), 8.638-8.659 (d, 2H, H-4, 5  $J$ =8.4Hz), 8.008-8.046 (t, 2H, H-3, 6  $J$ =15.2Hz), 7.862-7.883 (d, 1H, H-1, 8  $J$ =8.4Hz), 6.685-6.691 (d, 1H, H-5'  $J$ =14Hz), 6.715 (s, 1H, H-3'), 7.780-7.802 (d, 1H, H-6'  $J$ =8.8Hz).

## DISCUSSION

Acetylcholinesterase enzyme active site is divided into two main regions i.e. PAS and CAS. PAS have different aminoacids including Tyr72, Asp74, Tr124, Trp286 and Tyr341. CAS has divided in sub regions with Trp86, Gly121, Gly122, Tyr133, Ser203, Ala204, Phe295, Phe297, Glu334, Tyr337, Phe338 and His447 (Gocer *et al.*, 2016; Cheng *et al.*, 2017; Sukumaran *et al.*, 2018).



**Scheme 1:** Synthesis of PS12

For docking studies, five different standards were used in which four are FDA approved drugs (Bacalhau *et al.*, 2016; Goschorska *et al.*, 2019) and among them one is acridine derivative. All standards occupied the standard binding area as mentioned above. Derivatives for synthesis were selected on the basis of least binding energies that docked poses attained during docking study. Interactions of derivatives were checked in the form of hydrogen bonding, hydrophobic, pi-pi ( $\pi$ - $\pi$ ) and pi-CH ( $\pi$ -CH) interactions.

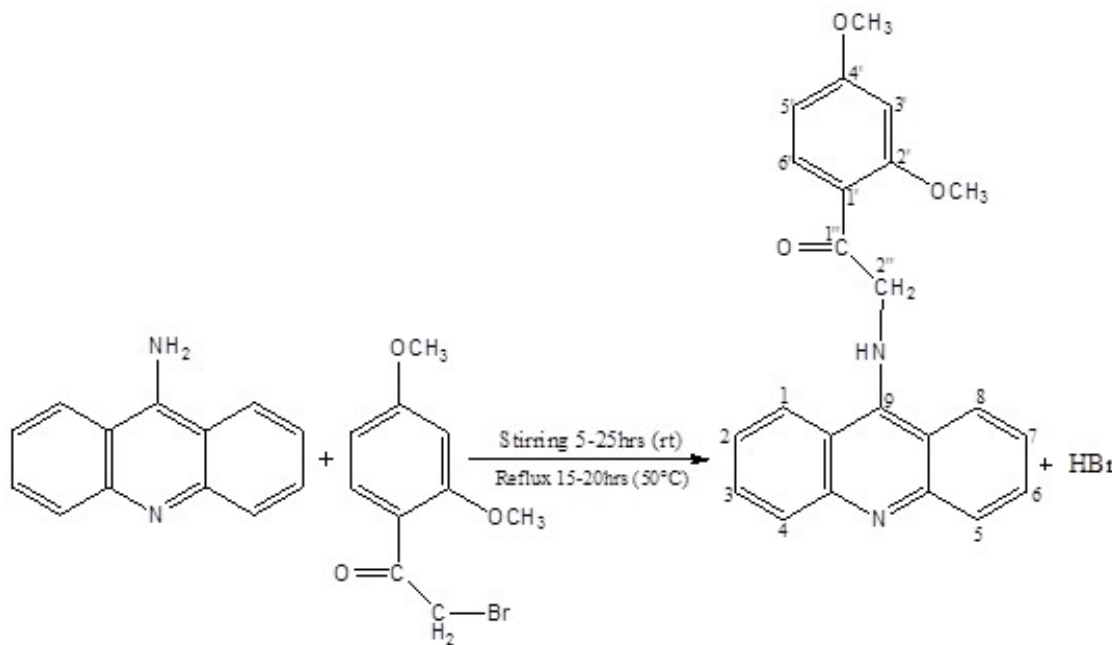
PS12 is phenacyl derivative having *para* phenyl group. In MOE, amine of acridine creating hydrogen bond with Gly120,  $\pi$ - $\pi$  stacking presented with Trp86 and Tyr341 and amino acid residues Asp74, Trp286, Tyr337, Phe338 and Tyr341 were part of hydrophobic interactions. Presence of *ortho*, *para* methoxy groups in PS13 increased the numbers of hydrogen bonding i.e. one with Phe295 and two with Arg296 while  $\pi$ - $\pi$  stacking and hydrophobic interactions were almost similar to PS12 (table 1, fig. 1 & 3). The interacting residues are common with standard drugs; however, interaction type is varied with molecular structure.

According to AutoDock results of PS12, hydroxyl of Ser125 is interacting with nitrogen of acridine ring via hydrogen bond. Tyr341 is involved in  $\pi$ - $\pi$  and  $\pi$ -CH interaction. Asp74, Trp86, Trp286, Phe338 and Tyr341 making hydrophobic interactions with ligand. In case of

PS13, four hydrogen bonds were observed involving central ring nitrogen and 9-amino of ligand with hydroxyl of Tyr337, carbonyl of Ser125 and amine of Trp86. Face to edge ( $\pi$ -CH) interaction occurred with Tyr341. Hydrophobic area is created by Asp74, Trp86, Phe297 and Tyr124 (table 1, fig. 2 & 4).

Both derivatives showed hydrogen bonds with the hotspot residues similar to standards with some additional interactions in both PAS and CAS region. Different amino acids were engaging the phenyl substitution, linking chain and acridine amines in hydrogen bonding. MOE and Auto Dock presented greater number of hydrogen bonds with the participation of nitrogen of acridine ring, acridine amine, phenacyl (connecting) moiety and substitution on phenyl ring. Standards and ligands interacted with PAS and CAS by  $\pi$ - $\pi$  and  $\pi$ -CH interactions with the contribution of Tyr341 is common with both softwares. Maximum number of hydrophobic interactions presented in ligand-target complex formation and played important role in capturing the acridine and terminal aromatic ring to fix with Asp74, Leu76, Trp86, Tyr124, Trp286, Phe297, Tyr337, Phe338 and Tyr341 as mostly presented hot spot residues (table 1).

Similar to the standards, ligands were also bind in the entrance of the target i.e. PAS due to this they are capable to inhibit entrance of acetylcholine in acetylcholinesterase and acetylcholine hydrolysis can be inhibited. On the



**Scheme 2:** Synthesis of PS13

other hand, those derivatives which bind to CAS similar to standards would be able to inhibit binding of acetylcholine at catalytic site of the enzyme. PAS and CAS bonded ligands considered as dual inhibitors. It is suggested that inhibition of acetylcholine hydrolysis by blocking acetylcholinesterase, increases the level of neurotransmitter in the brain and helps to improve cognitive function.

During investigation of enzyme inhibitory ability, PS12 showed good  $IC_{50}$  value as compared to PS13 (table 2). This difference in  $IC_{50}$  values can be correlated with the type and position of substitution at phenyl ring. Presence of *para* phenyl ring increased the potential of PS12 more than ten times as compared to PS13 having *ortho* and *para* methoxy groups. Enzyme inhibitory potentials of compounds are fully justified with their *insilico* findings where PS12 also presented good binding energy as compared to PS13.

Oxidative stress plays a fundamental role in AD pathogenesis by increased reactive oxygen species (ROS) indices in the regions of the brain affected by neurodegeneration (Youssef *et al.*, 2018; Goschorska *et al.*, 2019) and starts early aggregation of A $\beta$  and tau protein (Ademosun *et al.*, 2016; Shaik *et al.*, 2016).

Synthesized compounds exhibited significant antioxidant activity in terms of  $IC_{50}$  values (table 2). PS12 demonstrated better result than PS13. Significant antioxidant activity of PS12 supports enzyme inhibitory potential of this compound.

Protein amyloid aggregation is one of the reason of Alzheimer's disease and other 20 or more human diseases. Protein deposits (amyloid fibrils) actually the conversion of a soluble natural protein into insoluble form with primary and tertiary structures of different size in organs and tissues. Cell impairment and death also due to protein aggregated in different cell types. This concept becomes a reason to investigate A $\beta$  oligomers neurotoxicity in Alzheimer's disease. By amyloid toxicity membrane permeability increases with disruption integrity, formation of ion channels, oxidative stress and deregulation of cell homeostasis by its intracellular accumulation (Gazova *et al.*, 2008). To improves cognitive decline, fibril formation inhibition or disaggregation supposed to be one of the target therapy (Basiri *et al.*, 2017; Liu *et al.*, 2014). To prevent the formation of amyloid fibrils or deposits or to break them down once formed would be the ultimate goal. Synthesized derivatives were tested for disaggregation of fibrils at concentrations which showed inhibition of acetylcholinesterase. Congo red is used as a red dye to form complex with fibrils and indicates its presence. The maximum absorbance ( $\lambda_{max}$ ) of Congo red was recorded at 497.5nm. Fibrils synthesis was confirmed with the help of CR and showed  $\lambda_{max}$  at 513nm without CR appeared at 273.5nm. The quantity of fibrils reduces when disaggregation happens and fewer amounts of fibrils are available to bind with CR. This disaggregation is confirmed by peak shift. All compounds showed absorbance peak between 513-515nm, no significant peak shift from fibrils, indicated no disaggregation at these concentrations. All derivatives did not show disaggregation ability at the tested doses (table 2).

**Table 1:** Docking Scores of Standards, Parent and Top Ranked Ligands for synthesis

| S. No. | Standards      | Docking Scores MOE | Docking Autodock Vina | Hydrogen Bonds MOE | Bonds Autodock Vina | Hydrogen CH Stacking MOE | CH Stacking Autodock Vina | $\pi\text{-}\pi$ and $\pi\text{-}CH$ Stacking MOE | $\pi\text{-}\pi$ and $\pi\text{-}CH$ Stacking Autodock Vina | Hydrophobic Interaction/s MOE | Hydrophobic Interaction/s Autodock Vina |
|--------|----------------|--------------------|-----------------------|--------------------|---------------------|--------------------------|---------------------------|---|---|-------------------------------|---|
| 1.     | Tacrine        | -5.60              | -8.5                  | Tyr124             | Tyr124              | -                        | -                         | Tyr337  | Tyr337  | Tyr341                        | Tyr341                                  |
| 2.     | Donepezil      | -8.86              | -11.3                 | Phe295 Tyr337      | Phe295 Tyr124       | Tyr337                   | Tyr286                    | Tyr337, Phe297, Tyr341, His447                    | Tyr337, Phe338, Tyr341, His447                              | Tyr337, Phe338, Tyr341        | Tyr337, Phe338, Tyr341                  |
| 3.     | Galantamine    | -6.92              | -8.9                  | Gly121 Gly122      | Ser125 Glu202       | Ser203 His447            | -                         | Tyr337  | Tyr337  | Tyr341                        | Tyr341                                  |
| 4.     | Phystostigmine | -6.95              | -8.5                  | Tyr124 Tyr133      | Tyr124 Tyr341       | Tyr341                   | Glu202                    | Tyr337, Phe338, His447                            | Tyr337, Phe338, His447                                      | Tyr337                        | Tyr337                                  |
| 5.     | Rivastigmine   | -6.65              | -7.6                  | Phe295             | Tyr124 Ser125       | Tyr337 Phe338            | Tyr337                    | Tyr337, Phe338, Tyr341                            | Tyr337, Phe338, Tyr341                                      | Tyr337, Phe338, Tyr341        | Tyr337, Phe338, Tyr341                  |
| 6.     | 9AA            | -5.46              | -8.6                  | Tyr124 Ser125      | Tyr124              | -                        | Tyr337                    | Tyr337, Phe338, Tyr341                            | Tyr337, Phe338, Tyr341                                      | Tyr337, Phe338, Tyr341        | Tyr337, Phe338, Tyr341                  |
| 7.     | PS12           | -8.65              | -12.7                 | Gly120             | Ser125              | Tyr341                   | Tyr341                    | Tyr337, Phe338, Tyr341                            | Tyr337, Phe338, Tyr341                                      | Tyr337                        | Tyr337                                  |
| 8.     | PS13           | -6.90              | -10.1                 | Phe295 Arg296      | Trp86 Ser125        | Tyr341                   | Tyr341                    | Leu76, Trp286, Phe338, Tyr341, Tyr337             | Leu76, Trp286, Phe338, Tyr341, Tyr337                       | Asp74, Trp86, Phe297, Tyr124  | Asp74, Trp86, Phe297, Tyr124            |

\*Common residues among two softwares are highlighted

**Table 2:** Biological Activity of 9AA Derivatives

| S. No. | Compounds Code | ACHe IC <sub>50</sub> ± SD (μM) | Antioxidant IC <sub>50</sub> ± SD (μM) | Amyloid Disaggregation |
|--------|----------------|---------------------------------|--|------------------------|
| 1.     | PS12           | 2.400 ± 0.0482                  | 0.235 ± 0.0036                         | -                      |
| 2.     | PS13           | 26.138 ± 1.0327                 | 0.583 ± 0.0238                         | -                      |
| 3.     | 9AA            | 152.54 ± 0.4342                 | 121.57 ± 0.3637                        | -                      |
| 4.     | Galantamine    | 60.800 ± 0.4910                 | -                                      | -                      |
| 5.     | Ascorbic acid  | -                               | 3.05 ± 0.0605                          | -                      |

## CONCLUSION

In this study we successfully designed phenacyl based 9-aminoacridine analogues as potent antialzheimer's agents having significant AChE inhibition and antioxidant activity. They did not show any amyloid disaggregation at the tested dose. Present research investigations suggest that these two compounds can be considered very promising hit compounds offered an attractive starting point for further optimization in the drug-discovery process against AD.

## ACKNOWLEDGMENTS

Authors would like to acknowledge Higher Education Commission (HEC), Pakistan for funding the research study (NRPU research project number-6632).

## REFERENCES

Alzheimer's Association (2017). 2017 Alzheimer's disease facts and figures. *Alzheimer's & Dementia*, **13**(4): 325-373.

Acosta C, Anderson HD and Anderson CM (2017). Astrocyte dysfunction in Alzheimer disease. *J. Neurosci. Res.*, **95**(12): 2430-2447.

Ademosun AO, Oboh G, Bello F and Ayeni PO (2016). Antioxidative properties and effect of quercetin and its glycosylated form (Rutin) on acetylcholinesterase and butyrylcholinesterase activities. *Journal of Evidence-Based Complementary & Alternative Medicine*, **21**(4): NP11-NP17.

Ado MA, Abas F, Ismail IS, Ghazali HM and Shaari K (2015). Chemical profile and antiacetylcholinesterase, antityrosinase, antioxidant and  $\alpha$ -glucosidase inhibitory activity of *Cynometra cauliflora* L. leaves. *J. Sci. Food Agric.*, **95**(3): 635-642.

Aksu K, Ozgeris B, Taslimi P, Naderi A, Gülcin İ and Göksu S (2016). Antioxidant activity, acetylcholinesterase, and carbonic anhydrase inhibitory properties of novel ureas derived from phenethylamines. *Arch. Pharm.*, **349**(12): 944-954.

Ambure P, Kar S and Roy K (2014). Pharmacophore mapping-based virtual screening followed by molecular docking studies in search of potential acetylcholinesterase inhibitors as anti-Alzheimer's agents. *Biosystems*, **116**: 10-20.

Anand P and Singh B (2013). A review on cholinesterase inhibitors for Alzheimer's disease. *Arch. Pharmacal. Res.*, **36**(4): 375-399.

Aouani I, Sellami B, Lahbib K, Cavalier JF and Touil S (2017). Efficient synthesis of novel dialkyl-3-cyanopropylphosphate derivatives and evaluation of their anticholinesterase activity. *Bioorg. Chem.*, **72**: 301-307.

Bacalhau P, San Juan AA, Goth A, Caldeira AT, Martins R and Burke AJ (2016). Insights into (S)-rivastigmine inhibition of butyrylcholinesterase (BuChE): Molecular docking and saturation transfer difference NMR (STD-NMR). *Bioorg. Chem.*, **67**: 105-109.

Basiri A, Xiao M, McCarthy A, Dutta D, Byrareddy SN and Conda-Sheridan M (2017). Design and synthesis of new piperidone grafted acetylcholinesterase inhibitors. *Bioorg. Med. Chem. Lett.*, **27**(2): 228-231.

Begum S, Nizami SS, Mahmood U, Masood S, Iftikhar S and Saied S (2018). *In-vitro* evaluation and in-silico studies applied on newly synthesized amide derivatives of N-phthaloylglycine as Butyrylcholinesterase (BChE) inhibitors. *Comput. Biol. Chem.*, **74**: 212-217.

Borovlev IV, Demidov OP, Amangasieva GA and Avakyan EK (2016). Direct and facile synthesis of 9-aminoacridine and acridin-9-yl-ureas. *Tetrahedron Lett.*, **57**(32): 3608-3611.

Brogi S, Butini S, Maramai S, Colombo R, Verga L, Lanni C, De Lorenzi E, Lamponi S, Andreassi M, Bartolini M, Andrisano V, Novellino E, Campiani G, Brindisi M, Gemma S and Matteo PS (2014). Disease-Modifying Anti-Alzheimer's Drugs: Inhibitors of Human Cholinesterases Interfering with  $\beta$ -Amyloid Aggregation. *CNS Neurosci. Ther.*, **20**: 624-632.

Cavdar H, Senturk M, Guney M, Durdagi S, Kayik G, Supuran CT and Ekinci D (2019). Inhibition of acetylcholinesterase and butyrylcholinesterase with uracil derivatives: kinetic and computational studies. *J. of Enzyme Inhib. Med. Chem.*, **34**(1): 429-437.

Chen CLH, Sharma PR, Tan BY, Low C and Venketasubramanian N (2019). The Alzheimer's disease THerapy with NEuroaid (ATHENE) study protocol: Assessing the safety and efficacy of Neuroaid II (MLC901) in patients with mild-to-moderate Alzheimer's disease stable on cholinesterase inhibitors or memantine A randomized, double-blind, placebo-controlled trial. *Alzheimer's & Dementia: Translational Research & Clinical Interventions*, **5**: 38-45.

Chen YJ, Zheng HY, Huang XX, Han SX, Zhang DS, Ni JZ and He XY (2016). Neuroprotective Effects of Icariin on Brain Metabolism, Mitochondrial Functions, and Cognition in Triple-Transgenic Alzheimer's Disease Mice. *CNS Neurosci. Ther.*, **22**(1): 63-73.

Cheng S, Song W, Yuan X and Xu Y (2017). Gorge Motions of Acetylcholinesterase Revealed by Microsecond Molecular Dynamics Simulations. *Scientific Reports*, **7**(1): 3219.

Christoph R, Markus M and Kerber A (2004). QSPR Using MOLGEN-QSPR: The Example of Haloalkane Boiling Points. *J. Chem. Inf. Comput. Sci.*, **44**(6): 2070-2076.

Ellman GL, Courtney KD, Andres V and Featherstone RM (1961). A new and rapid colorimetric determination of acetylcholinesterase activity. *Biochem. Pharmacol.*, **7**(2): 88-95.

Fernández S, Giglio J, Reyes AL, Damián A, Pérez C, Pérez DI, Gonzalez M, Oliver P, Rey A, Engler H and Cerecetto H (2017). 3-(Benzylxyloxy)-1-(5- $\text{F}^{18}$

F]fluoropentyl)-5-nitro-1 *H*-indazole: A PET radiotracer to measure acetylcholinesterase in brain. *Future Med. Chem.*, **9**(10): 983-994.

Gazova Z, Bellova A, Daxnerova Z, Imrich J, Kristian P, Tomascikova J, Bagelova J, Fedunova D and Antalik M (2008). Acridine derivatives inhibit lysozyme aggregation. *Eur. Biophysics J.*, **37**(7): 1261-1270.

Gellerman G (2012). Recent Synthetic Approaches to Anti-cancer 9-Anilinoacridines. A Review. *Org. Prep. and Proced. Int.*, **44**(3): 187-221.

Gensicka-Kowalewska M, Cholewinski G and Dzierzbicka K (2017). Recent developments in the synthesis and biological activity of acridine/acridone analogues. *RSC Adv.*, **7**(26): 15776-15804.

Gocer H, Topal F, Topal M, Küçük M, Teke D, Gülçin İ, Alwasel SH and Supuran CT (2015). Acetylcholinesterase and carbonic anhydrase isoenzymes I and II inhibition profiles of taxifolin. *J. Enzyme Inhib. Med. Chem.*, **31**(3): 441-447.

Goschorska M, Gutowska I, Baranowska-Bosiacka I, Piotrowska K, Metryka E, Safranow K and Chlubek D (2019). Influence of Acetylcholinesterase Inhibitors Used in Alzheimer's Disease Treatment on the Activity of Antioxidant Enzymes and the Concentration of Glutathione in THP-1 Macrophages under Fluoride-Induced Oxidative Stress. *Int. J. Environ. Res. Public Health*, **16**(1): 10.

Halgren TA (1996). Merck molecular force field. II. MMFF94 van der Waals and electrostatic parameters for intermolecular interactions. *J. Comput. Chem.*, **17**(5-6): 520-552.

Halgren TA (1999). MMFF VI. MMFF94s option for energy minimization studies. *J. Comput. Chem.*, **20**(7): 720-729.

Inestrosa NC, Dinamarca MC and Alvarez A (2008). Amyloid-cholinesterase interactions. *FEBS J.*, **275**(4): 625-632.

Jacob RB, Andersen T and McDougal OM (2012). Accessible High-Throughput Virtual Screening Molecular Docking Software for Students and Educators. *PLoS Comput. Biol.*, **8**(5): e1002499.

Jannat S, Balupuri A, Ali MY, Hong SS, Choi CW, Choi YH, Ku JM, Kim WJ, Leem JY, Kim JE, Shrestha AC, Ham HN, Lee KH, Kim DM, Kang NS and Park GH (2019). Inhibition of  $\beta$ -site amyloid precursor protein cleaving enzyme 1 and cholinesterases by pterosins via a specific structure-activity relationship with a strong BBB permeability. *Exp. Mol. Med.*, **51**(2): 12.

Johnson G, and Moore S (2006). The Peripheral Anionic Site of Acetylcholinesterase: Structure, Functions and Potential Role in Rational Drug Design. *Curr. Pharm. Des.*, **12**(2): 217-225.

Korabecny J, Musilek K, Holas O, Binder J, Zemek F, Marek J, Pohanka M, Opletalova V, Dohnal V and Kuca K (2010). Synthesis and in vitro evaluation of N-alkyl-7-methoxytacrine hydrochlorides as potential cholinesterase inhibitors in Alzheimer disease. *Bioorg. Med. Chem. Lett.*, **20**(20): 6093-6095.

Kristofikova Z, Ricny J, Soukup O, Korabecny J, Nepovimova E, Kuca K, and Ripova D (2017). Inhibitors of Acetylcholinesterase Derived from 7-Methoxytacrine and Their Effects on the Choline Transporter CHT1. *Dement. Geriatr. Cogn. Disord.*, **43**(1-2): 45-58.

Liu J, Qiu J, Wang M, Wang L, Su L, Gao J, Gu Q, Xu J, Huang SL, Gu LQ, Huang ZS and Li D (2014). Biochimica et Biophysica Acta Synthesis and characterization of  $^1\text{H}$ -phenanthro [9, 10- d] imidazole derivatives as multifunctional agents for treatment of Alzheimer's disease. *BBA-General Subjects*, **1840**(9): 2886-2903.

Lopez-Vallejo F, Caulfield T, Martinez-Mayorga K, Julianotti M, Nefzi A, Houghten R and Medina-Franco J (2011). Integrating Virtual Screening and Combinatorial Chemistry for Accelerated Drug Discovery. *Comb. Chem. High Throughput Screening*, **14**(6): 475-487.

Manivannan C, Sundaram KM, Renganathan R and Sundararaman M (2012). Investigations on Photoinduced Interaction of 9-Aminoacridine with Certain Catechols and Rutin. *J. Fluoresc.*, **22**(4): 1113-1125.

Meng XY, Zhang HX, Mezei M and Cui M (2011). Molecular Docking: A Powerful Approach for Structure-Based Drug Discovery. *Curr. Comput.-Aided Drug Des.*, **7**(2): 146-157.

Mohammadi-Khanaposhtani M, Saeedi M, Zafarghandi NS, Mahdavi M, Sabourian R, Razkenari EK, Alinezhad H, Khanavi M, Foroumadi A, Shafiee A and Akbarzadeh T (2015). Potent acetylcholinesterase inhibitors: Design, synthesis, biological evaluation, and docking study of acridone linked to 1,2,3-triazole derivatives. *Eur. J. Med. Chem.*, **92**: 799-806.

Muhammad SA and Fatima N (2015). In silico analysis and molecular docking studies of potential angiotensin-converting enzyme inhibitor using quercetin glycosides. *Pharmacogn. Mag.*, **11**(Suppl 1): S123-6.

Narla RS, and Rao MNA (1995). Scavenging of Free-radicals and Inhibition of Lipid Peroxidation by 3-Phenylsydnone. *J. Pharm. Pharmacol.*, **47**(8): 623-625.

Nwidu LL, Elmorsy E, Thornton J, Wijamanige B, Wijesekara A, Tarbox R, Warren A and Carter WG (2017). Anti-acetylcholinesterase activity and antioxidant properties of extracts and fractions of *Carpolobia lutea*. *Pharm. Biol.*, **55**(1): 1875-1883.

Peauger L, Azzouz R, Gembus V, Tıntaş ML, Sopková-de Oliveira Santos J, Bohn P, Papamicael C and Levacher V (2017). Donepezil-Based Central Acetylcholinesterase Inhibitors by Means of a "Bio-Oxidizable" Prodrug Strategy: Design, Synthesis, and *in Vitro* Biological Evaluation. *J. Med. Chem.*, **60**(13): 5909-5926.

Rahman MM, Karim MR, Ahsan MQ, Khalipha ABR,

Chowdhury MR and Saifuzzaman M (2012). Use of computer in drug design and drug discovery: A review. *Int. J. Pharma. Life Sci.*, **1**(2): 1-21

Ramshini H, Ebrahim-Habibi A, Aryanejad S and Rad A (2015). Effect of cinnamomum verum extract on the amyloid formation of hen egg-white lysozyme and study of its possible role in Alzheimer's disease. *Basic Clin. Neurosci.*, **6**(1): 29-37.

Scotti L, Júnior FJBM, Ishiki HM, Ribeiro FF, Duarte MC, Santana GS, Oliveira TB, Diniz MFFM, Júnior LJQ and Scotti MT (2018). Computer-Aided Drug Design Studies in Food Chemistry. In: Natural and Artificial Flavoring Agents and Food Dyes. Handbook of Food Bioengineering, Academic press, pp.261-297.

Senol FS, Skalicka Woźniak K, Khan MTH, Erdogan Orhan I, Sener B and Główiāk K (2011). An *in vitro* and *in silico* approach to cholinesterase inhibitory and antioxidant effects of the methanol extract, furanocoumarin fraction and major coumarins of *Angelica officinalis* L. fruits. *Phytochemistry Letters*, **4**(4): 462-467.

Shaik JB, Palaka BK, Penumala M, Kotapati KV, Devineni SR, Eadlapalli S, Darla MM, Ampasala DR, Vadde R and Amooru GD (2016). Synthesis, pharmacological assessment, molecular modeling and *in silico* studies of fused tricyclic coumarin derivatives as a new family of multifunctional anti-Alzheimer agents. *Eur. J. of Med. Chem.*, **107**: 219-232.

Spilovska K, Korabecny J, Kral J, Horova A, Musilek K, Soukup O, Soukup O, Drtinova N, Gazova Z, Siposova K and Kuca K (2013). 7-methoxytacrine-adamantylamine heterodimers as cholinesterase inhibitors in Alzheimer's disease treatment synthesis, biological evaluation and molecular modeling studies. *Molecules*, **18**(2): 2397-2418.

Sukumaran SD, Faraj FL, Lee VS, Othman R and Buckle MJC (2018). 2-Aryl-3-(arylideneamino)-1,2-dihydroquinazoline-4(3 *H*)-ones as inhibitors of cholinesterases and self-induced  $\beta$ -amyloid (A $\beta$ ) aggregation: biological evaluations and mechanistic insights from molecular dynamics simulations. *RSC Adv.*, **8**(14): 7818-7831.

Tiwari P, Dwivedi S, Singh MP, Mishra R and Chandy A (2013). Basic and modern concepts on cholinergic receptor: A review. *Asian Pac. J. Trop. Dis.*, **3**(5): 413-420.

Venkatachalam H, Yogendra N and Jayashree BS (2012). Evaluation of the antioxidant activity of novel synthetic chalcones and flavonols. *Int. J. Chem. Eng.*, **3**(3): 216-219.

Weinstock M and Groner E (2008). Rational design of a drug for Alzheimer's disease with cholinesterase inhibitory and neuroprotective activity. *Chem.-Biol. Interact.*, **175**(1-3): 216-221.

www.rcsb.org.

Yang J, Zhang P, Hu Y, Liu T, Sun J and Wang X (2019). Synthesis and biological evaluation of 3-arylcoumarins as potential anti-Alzheimer's disease agents. *J. Enzyme Inhib. Med. Chem.*, **34**(1): 651-656.

Youssef KM, Fawzy IM and El-Subbagh HI (2018). N-substituted-piperidines as novel Anti-alzheimer agents: Synthesis, antioxidant activity and molecular docking study. *Future J. Pharm. Sci.*, **4**(1): 1-7.